Geol. Soc. Malaysia, Bulletin 36, December 1994; pp. 31-53

Depositional and diagenetic histories of reservoir sandstones in the Jerneh field, central Malay Basin

MAZLAN B. HJ. MADON

Petronas Research and Scientific Services Sdn. Bhd.
Lot 1026 PKNS Industrial Area
54200 Ulu Kelang
Malaysia

Abstract: The depositional and diagenetic histories of upper Miocene reservoir sandstones in the Jerneh field, Malay Basin, were interpreted from core and log data. The sandstones, at depths of between 1,250 and 2,000 m, were deposited during a middle to late Miocene regressive episode. Sandbodies characterize different facies associations: distributary mouthbar and shoreface sandbodies in the delta front, and channel point bar deposits in the delta plain facies association. Laterally continuous sheet sandstones characterize the shallow marine facies association which was deposited during transgression over the delta.

With increasing depth, the reservoir sandstones show a higher degree of compaction and quartz cementation, which resulted in reduced porosities ranging between 10% and 25%. An estimated 15% to 50% of the original depositional porosity was lost by compaction during shallow burial (< 1 km). Quartz overgrowths (1–7%) are interpreted to have started forming at depths of about 1,200 m, K-feldspar was selectively dissolved by acidic formation waters, while plagioclase remained relatively stable. The effect of dissolution, however, is thought to be insignificant in terms of porosity enhancement.

INTRODUCTION

This paper gives an interpretation of the depositional and diagenetic histories of the reservoir sandstones in the Jerneh field, offshore Peninsular Malaysia. The field is located in the centre of the Malay Basin (Fig. 1), and is now being developed by Esso Production Malaysia Inc. (EPMI).

The reservoir intervals in the field belong to seismic groups D and E (Fig. 2), which are important hydrocarbon producers in the central and northern Malay Basin. The sediments have been interpreted as lower coastal plain to tidal in origin, but no detailed description was given (e.g. Thambydurai *et al.*, 1988). Petrographic and diagenetic studies on this important group of reservoirs are also lacking. This paper discusses on these two aspects of the reservoir sandstones.

GEOLOGICAL SETTING

The Malay Basin is an elongated (NW-SE) intracratonic basin filled with Oligocene to Recent, mainly siliciclastic, sediments. The sedimentation history comprises three main phases: transgression (Oligocene-middle Miocene) - regression (middle Miocene-late Miocene) - transgression (Pliocene to Recent). In the southern part of the basin, tectonic deformation has caused inversion of the basin during middle to late Miocene and resulted in a regional base-Pliocene unconformity.

The late Miocene deformation produced numerous compressional anticlines which form the major hydrocarbon traps in the basin. The Jerneh field is one such structure: an east-west trending anticline, cut by a north-south fault at its western end (Fig. 3).

During the Miocene, the Malay Basin was a narrow gulf-like basin partially connected to the open ocean at its southeastern end. Studies by Nik Ramli (1988) have shown that late Oligocene to early Miocene sedimentation in the area was dominated by fan-deltas and deltas flanking the gulf. Paleocurrent analysis from dipmeter data suggest that the upper Miocene sequence in the Jerneh field was deposited in a southward-flowing alluvial-deltaic system along the axis of the basin. Analogy is drawn from the modern-day Lower Central Plains of Thailand, where there is a broad alluvial delta plain with rivers flowing southward and transverse alluvial fans at its margins (Fig. 4).

STRATIGRAPHY AND PALEOENVIRONMENTS

The strata penetrated in the Jerneh field are herein subdivided into three informal lithostratigraphic units: Jerneh, Bintang, and Pilong, in younging order (Fig. 2). The Jerneh and Bintang formations correspond approximately to EPMI's seismic units E and D, respectively, whereas the overlying Pilong formation (cf. Armitage and

Presented at GSM Annual Geological Conference '92

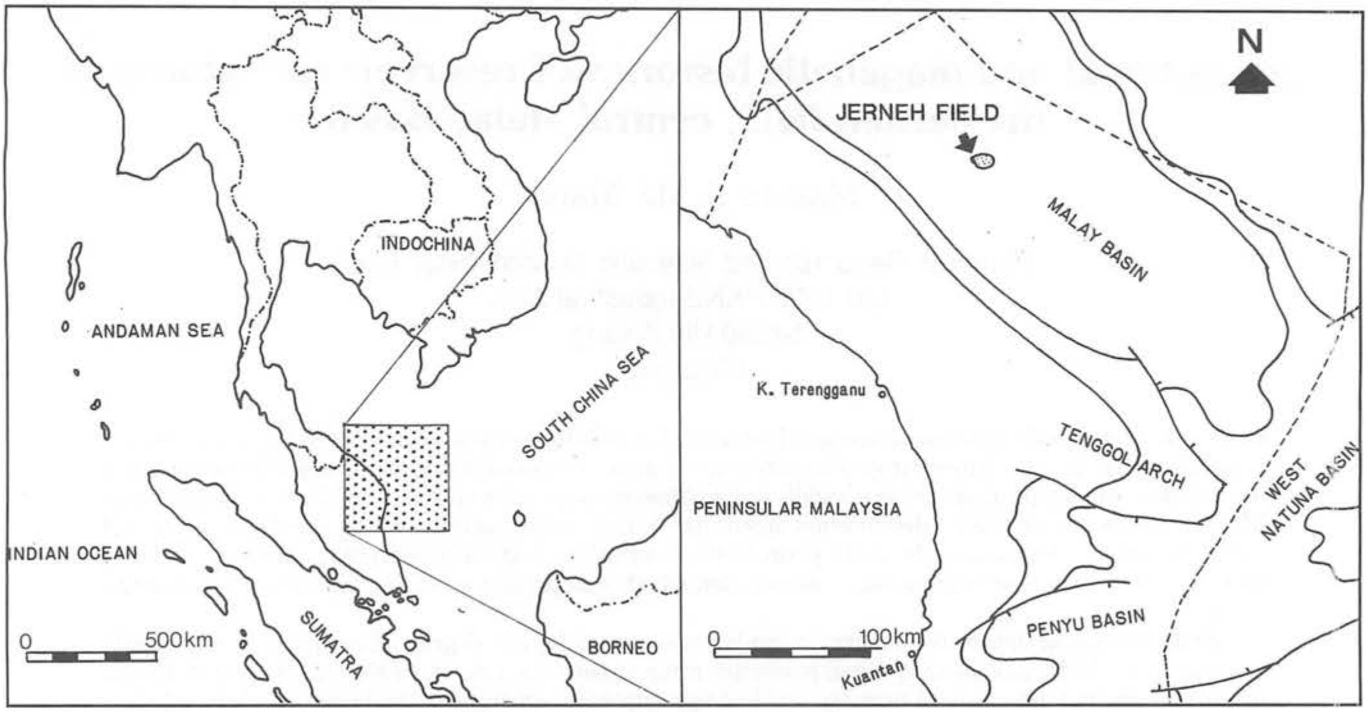

Figure 1. Location map of Jerneh field.

AGE	SEISMIC UNIT	FORMATION	RESERVOIR UNITS	DEPOSITIONAL ENVIRONMENTS
Pliocene	B	Pilong		shallow marine
Upper Miocene	D	Bintang	D-32 D-60	brackish shallow marine
	E	Jerneh	E-50 E-90	deltaic - nonmarine

Figure 2. Stratigraphy of the reservoir intervals in Jerneh-3. formation names are informal, based on lithostratigraphic analysis of several wells.

Viotti, 1977) corresponds to units A and B. Microfossil assemblages (unpublished data) suggest an upper Miocene age for Jerneh and Bintang formations, and Pliocene to Recent for Pilong formation.

Reservoir sandstones studied in this paper occur in the Jerneh and Bintang formations, at depths between 1,250 and 2,000 m.

Jerneh formation

Jerneh formation consists of fine-grained sandstone, mudstone, and coal. Its lower part is characterized by funnel-shaped SP log motifs (20–100 m thick), representing coarsening-upward units of mudstone, siltstone, and fine-grained sandstone (Fig. 5). Coal beds occur at the top of some coarsening-upward units. Foraminifers are rare,

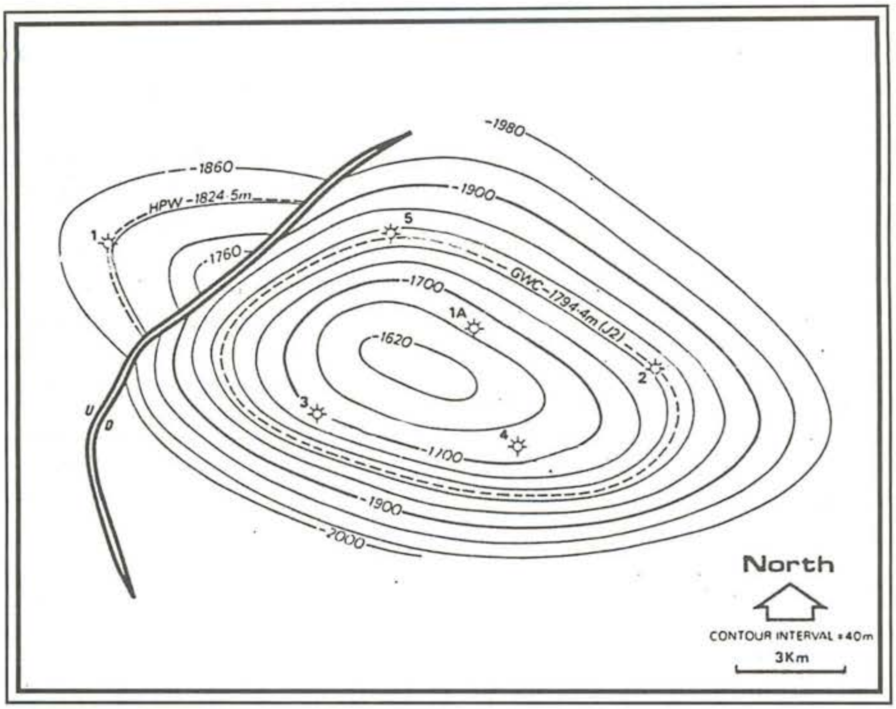

Figure 3. Simplified structural map of Jerneh field at E-50 sand level. From Thambydurai *et al.* (1988).

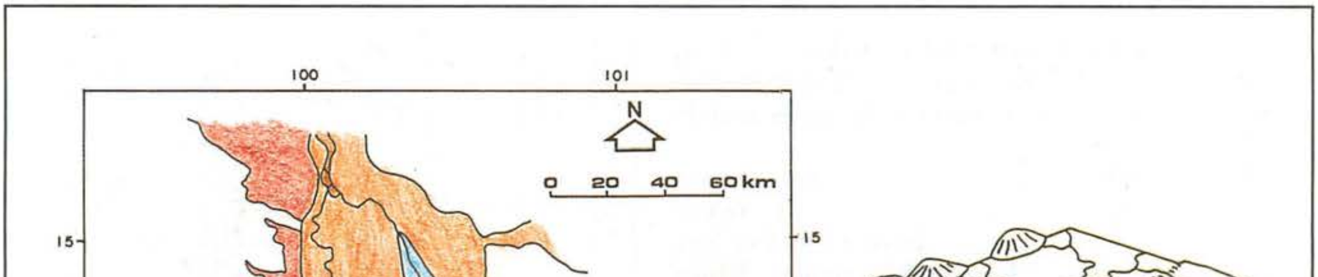

Figure 4. Map of Lower Central Plains, Thailand, showing the geomorphology of the Quaternary. Note the broad triangular area of alluvial deltaic deposits at the centre, flanked by alluvial fans coming off steep (faulted?) slopes. Modified after Thiramongkol (1983).

but palynomorphs, mainly freshwater type, are abundant.

The upper Jerneh has abundant coal beds, and commonly shows bell-shaped or blocky SP-log motifs about 20 m thick, representing fining-upward sandstone units. Samples of the interbedded shales yielded few nonmarine palynomorphs, but no foraminifers.

The occurrence of coal, sparse marine fauna, and the dominance of freshwater palynomorphs suggest that the Jerneh formation was deposited in a slightly marine-influenced coastal plain environment. The upward-coarsening units represent progradational sedimentation, probably in a deltaic setting. Fining-upward sandstone units in the upper part are interpreted as channel sandbodies.

Bintang formation

The Bintang formation consists of greenish grey glauconitic sandstones intercalated with laminated siltstones and shales. Glauconitic minerals occur mainly as sand-size structureless peloids and as thin coatings on detrital grains.

The lower part of Bintang formation consists of fine-grained glauconitic sandstone (15–30 m thick) interbedded with thinner mudstone (Fig. 5). Most of the sandstones show blocky or slightly funnel-shaped log motifs. The upper Bintang is mainly siltstone and shale.

Foraminifers, up to 30 specimens per sample, are dominated by *Ammonia* and fewer *Ammobaculites exiguus*. Pollen grains are dominated by the mangrove Rhizophora, which decreases upward.

The presence of glauconite, foraminifers, and mangrove pollen suggests deposition in a shallow marine environment. The sandstones are interpreted as shallow marine sand bars and tidal channel deposits. The lower abundance and diversity of foraminifers in the Bintang compared to the overlying Pilong formation indicates a brackish or restricted marine environment. The mudstones in the Bintang formation are interpreted as offshore marine muds.

FACIES ASSOCIATIONS AND SANDBODY TYPES

Detailed facies analysis using cores and well logs from three wells has enabled the recognition of sandbodies in three facies associations: the delta front and delta plain facies associations in the Jerneh formation, and the shallow marine facies association in the Bintang formation. These facies associations are described below.

Delta front facies association

This facies association consists of a coarsening-upward sequence of shale and siltstone at the base, becoming more sandy upward (Fig. 6). The coarsening-upward sequences exhibit funnel-shaped log character, and consists of lenticular mudstone overlain by wavy to flaser-bedded sandstone or parallel laminated sandstone. The lenticular mudstone contains some foraminifers. Coal bed occur above some of the sequences.

The lower part of Jerneh formation consists of stacked coarsening-upward sequences, each

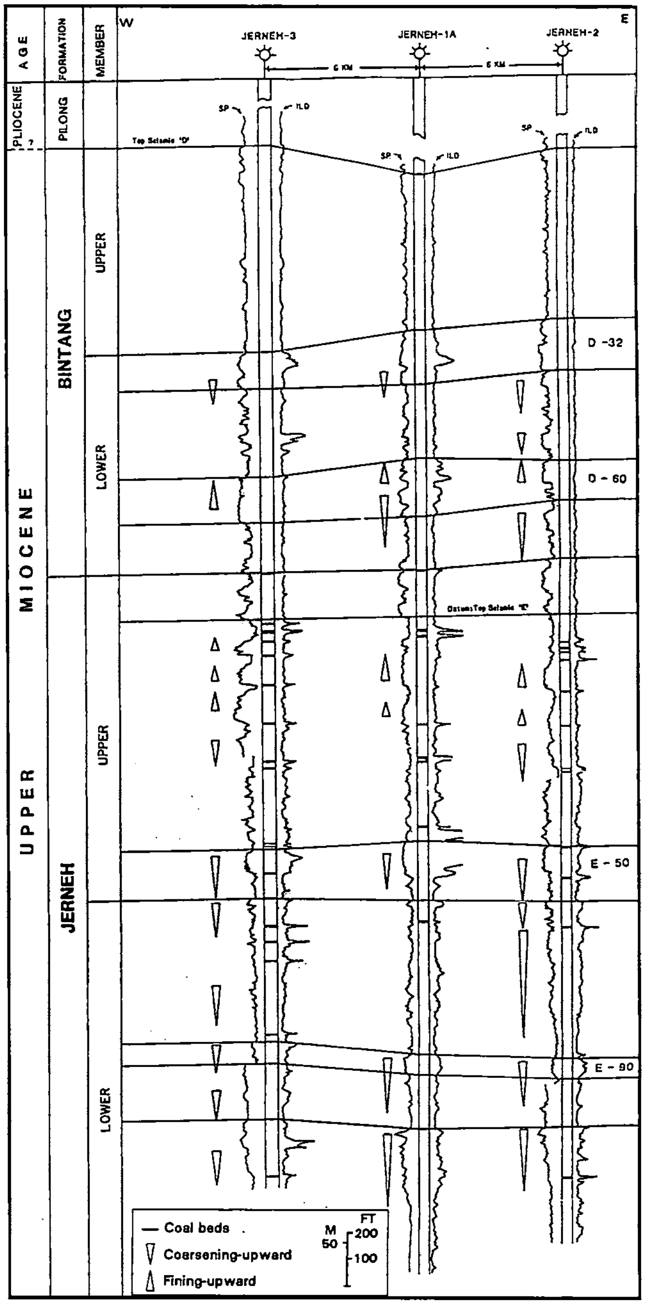

Figure 5. Lithostratigraphic correlation of the Jerneh wells, showing the major coarsening and fining upward sequences and the reservoir units studied petrographically.

measuring 15–20 m and extending across the entire field (Fig. 7). The sandstones have varying thicknesses.

Interpretation:

A coarsening-upward sequence indicates deposition in a prograding shoreline. The occurrence of foraminifers in the lower siltstone suggests that it was a marine shoreline; the siltstone representing prodelta to distal bar sediments deposited in a delta front environment. Bioturbation indicates a low-energy environment below wave base. The graded siltstone layers were probably deposited by density currents on the delta slope (Elliott, 1986). Slump structures indicate unstable delta slope conditions.

The parallel laminated sandstone facies (Fig. 6) is interpreted as a distributary mouth bar deposit formed of wave-reworked sand. Overlying the mouthbar-shoreface deposit is the heterolithic sandstone-mudstone facies which represents low energy deposits formed in the interdistributary areas.

Delta plain facies association

This facies association is typical of the upper Jerneh. Its consists essentially of several coarsening-upward and fining-upward units. The coarsening-upward unit consists of coal, overlain by rhythmite mudstone, which grades upward into lenticular, wavy, and flaser bedded heterolithic sandstone-mudstone facies (Fig. 8). The fining-upward unit consists of sharp-based, cross-laminated, flaser bedded sandstone which grades upward into lenticular mudstone, rootlet mudstone, and coal at the top (Fig. 9).

Interpretation

This facies association is interpreted to have been deposited on a delta plain because of the abundance of coal, the lack of marine fossils, and the dominance of freshwater or inland-plant derived pollen.

The coarsening-upward units were deposited by small lacustrine deltas or crevasse splays which prograded into subsiding peat swamps. Most coal

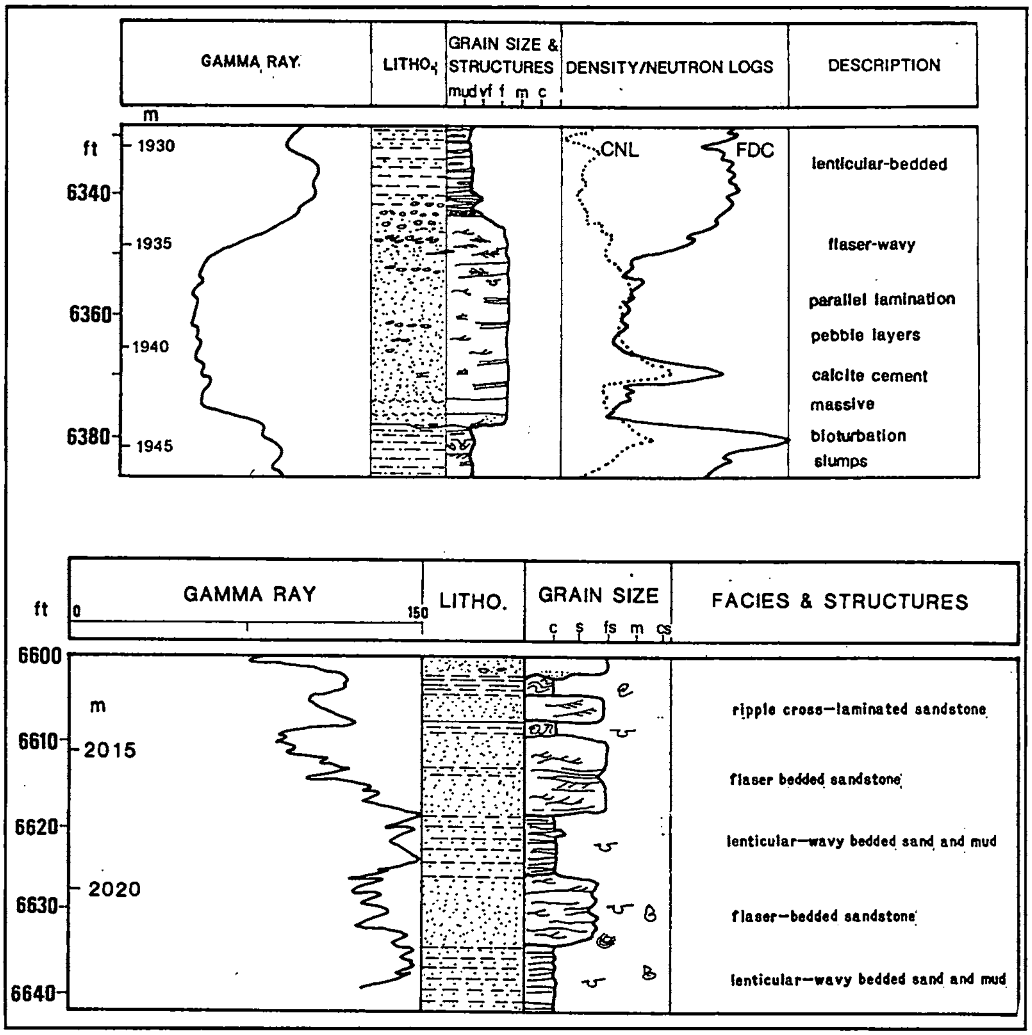

Figure 6. Delta front deposits from the lower Jerneh. See Figure 7 for the location of cores.

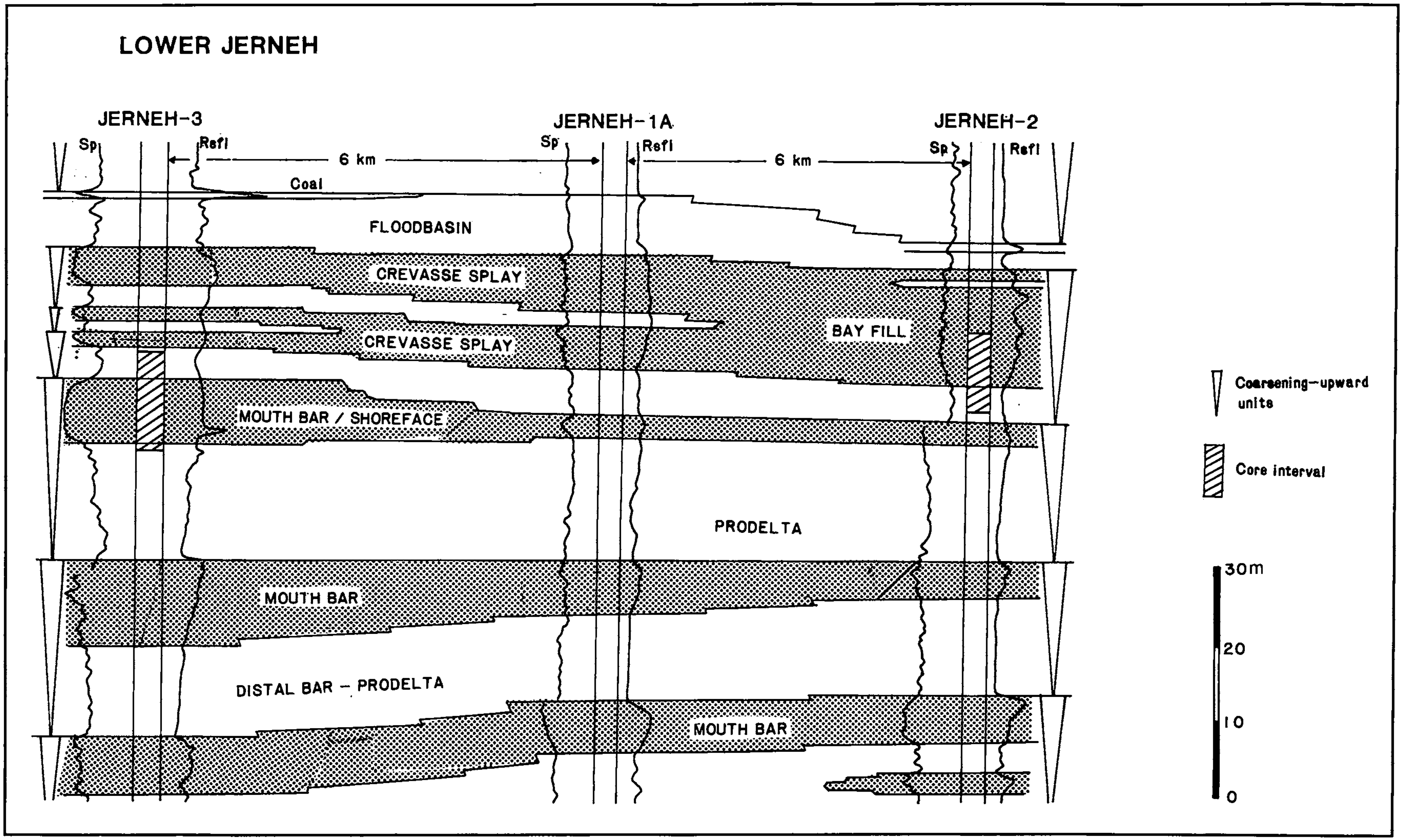

Figure 7. Correlation of sandbodies in lower Jerneh, showing the lateral continuity of delta front sandstones. Core intervals are shown in Figure 6.

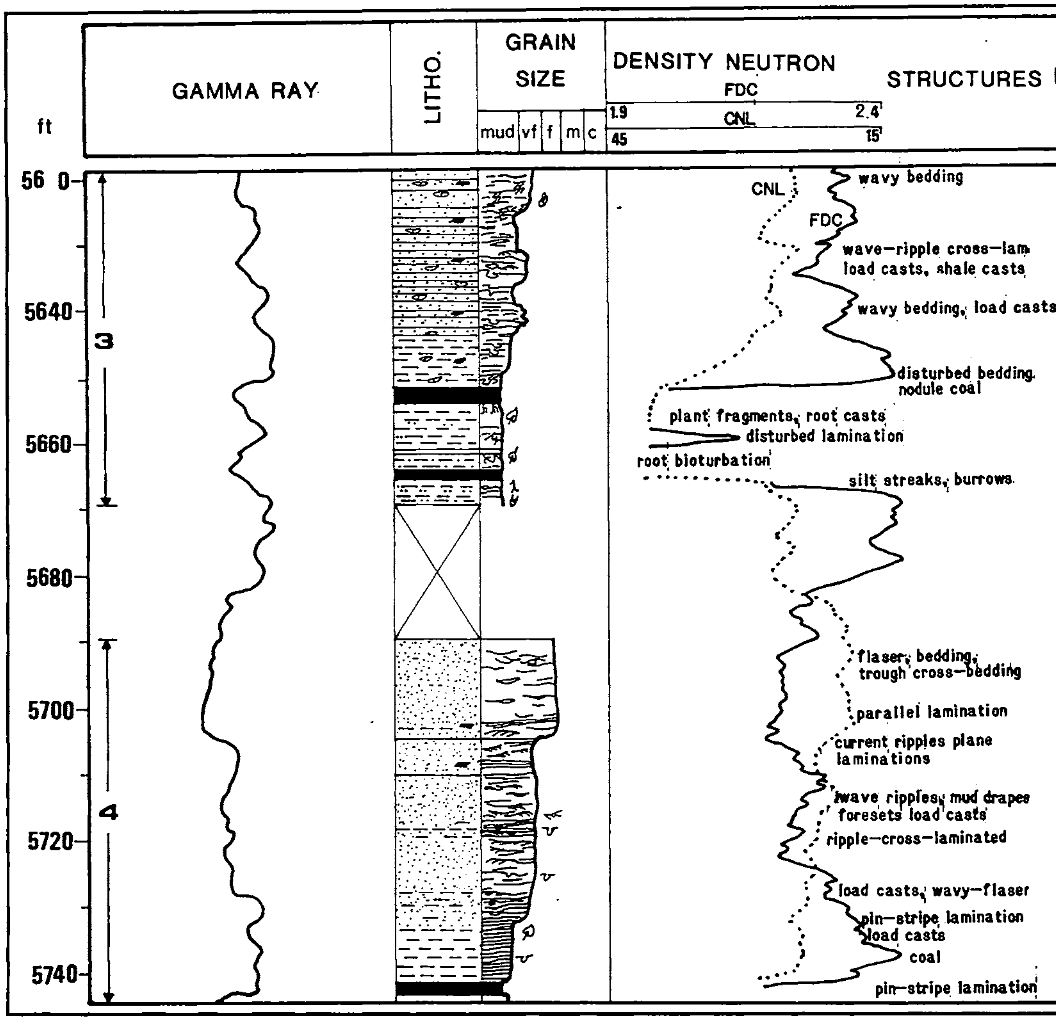

Figure 8. Core log of coarsening-upward sequences in the delta plain facies association (Jerneh-3 well). Each sequence comprises floodbasin or lacustrine deposits (coal, rhythmite) passing upward into heterolithic sandstone-mudstone facies representing crevasse splays and associated channels.

beds can be correlated across the field by wireline logs, and extend for more than 10 km (Fig. 10). They were probably deposited in swamps as a result of delta-lobe abandonment (Elliott, 1986).

The fining-upward sandstone units are interpreted as distributary channel point-bar deposits, based on their sharp basal contacts and fining-upward log character. The overlying rootlet mudstone and coal are interpreted as levees and overbank deposits, respectively.

Shallow marine facies association

This facies association typifies the Bintang formation. It consists of 5 to 50 m thick sandstones alternating with shale and siltstone (Fig. 11). Most of the sandbodies appear to be continuous laterally, while some occur over short distances. Glauconitic, flaser-bedded sandstones show slightly funnel-shaped log motifs, indicating upward-coarsening trends, whereas the cross-laminated sandstone shows blocky log responses, and appear to pinch out laterally (Fig. 5). Foraminifers are quite common in the siltstone and shale facies of the Bintang formation.

Interpretation:

This facies association is interpreted as shallow marine deposits because of the presence of glauconite and foraminifers in the intervening mudrocks. The glauconitic sandstone bodies are interpreted as offshore sand bars encased in shelf mudstones, analogous to those in the Duffy Mountain sandstone (Mancos Shale) of NW Colorado, described by Boyles and Scott (1982). The erosional base and lenticular nature of some sandbodies suggest that some may be subtidal channel deposits (Fig. 11).

DEPOSITIONAL HISTORY

The facies associations are interpreted to represent three phases of deltaic sedimentation (Fig. 12) in response to the interplay between rate of sedimentation and rate of subsidence (Curtis, 1970):

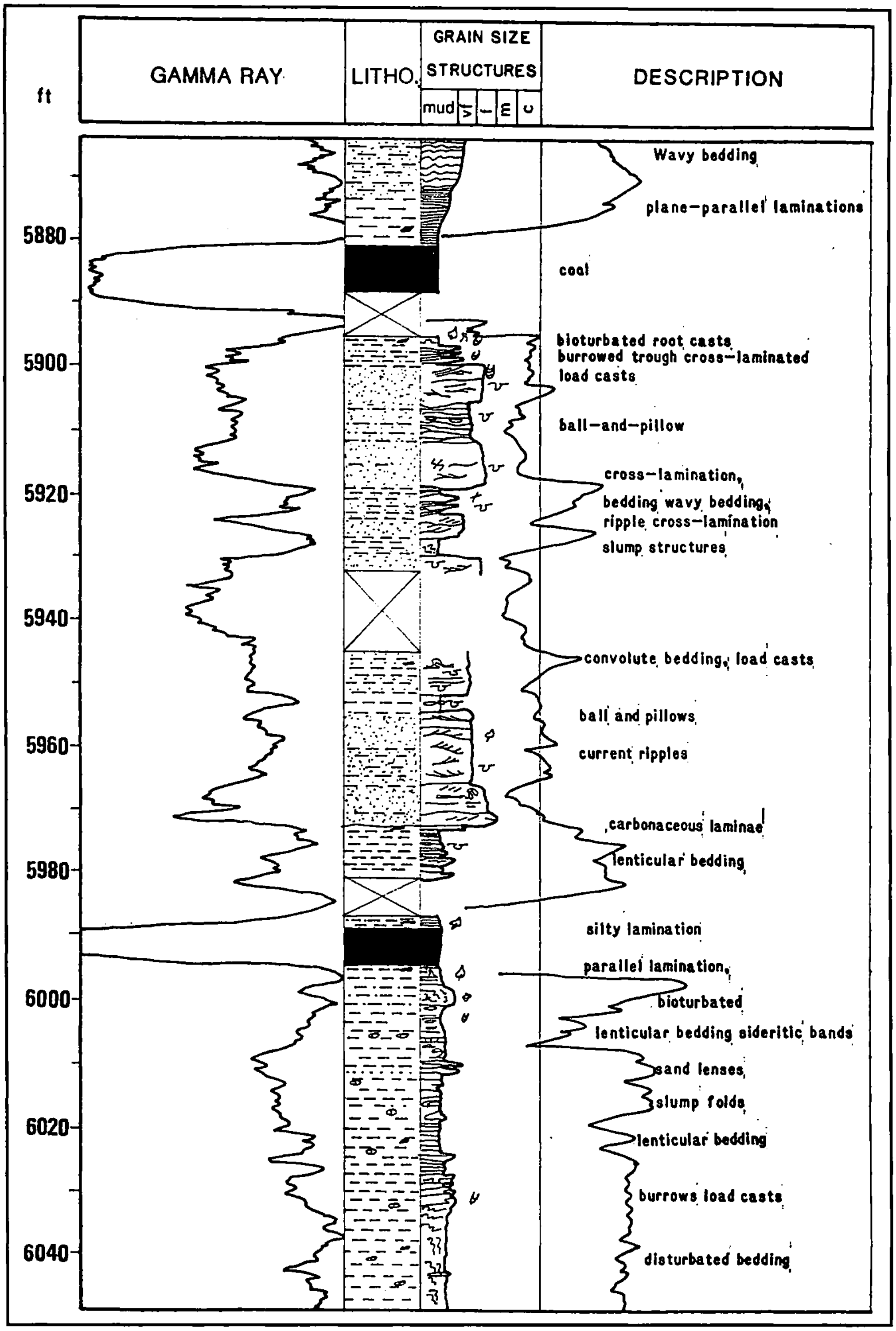

Figure 9. Core log from Jerneh-2 well, showing delta plain facies association comprising a coarsening-upward sequence of floodbasin-lacustrine deposits overlain by channel pointbar sandstones. The uppermost sandstone (@ 5,900 ft) fines upward into rootlet mudstone and coal, representing channel abandonment. The sequence in overlain by coal and rhythmite which represent floodbasin lacustrine deposits.

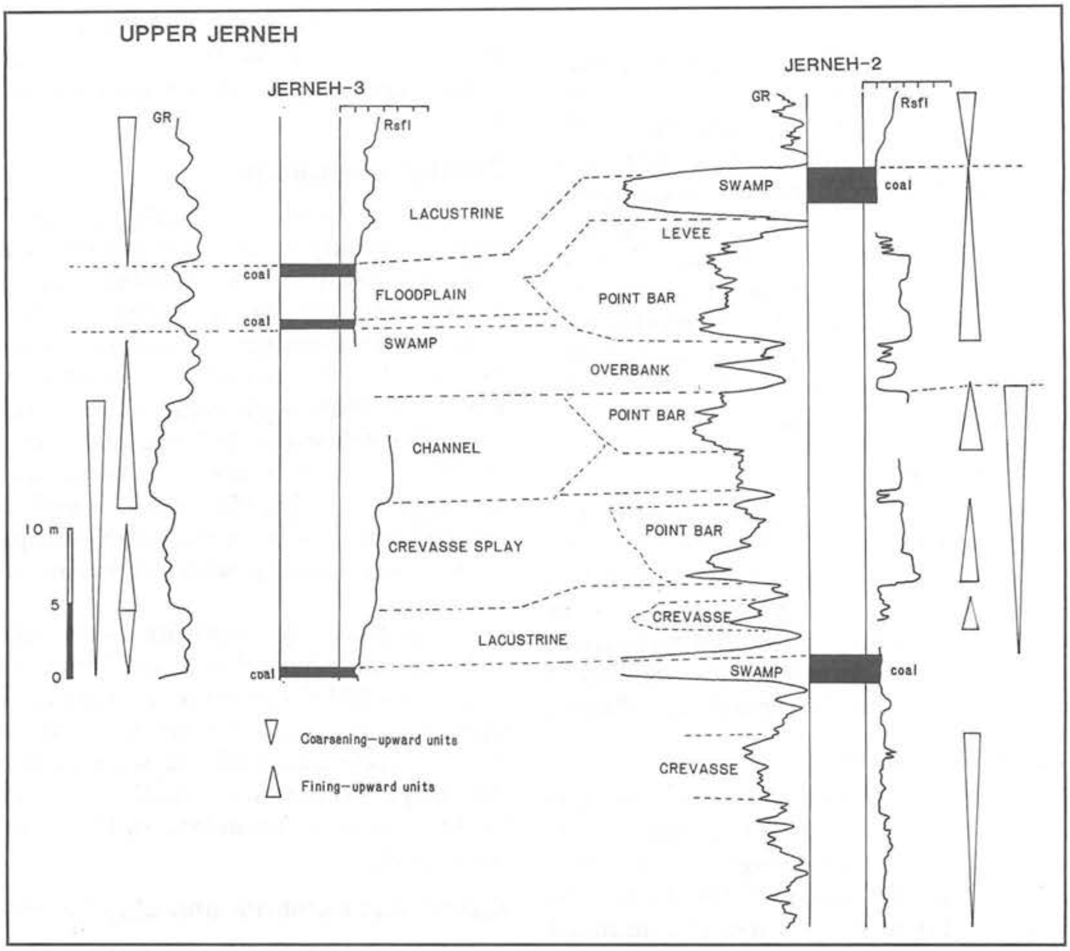

Figure 10. Correlation of the E-50 sandstone interval as logged in Figures 8 and 9. The coal beds are correlatable over a distance of more than 10 km. The intervening clastics, especially the channel deposits, are less continuous.

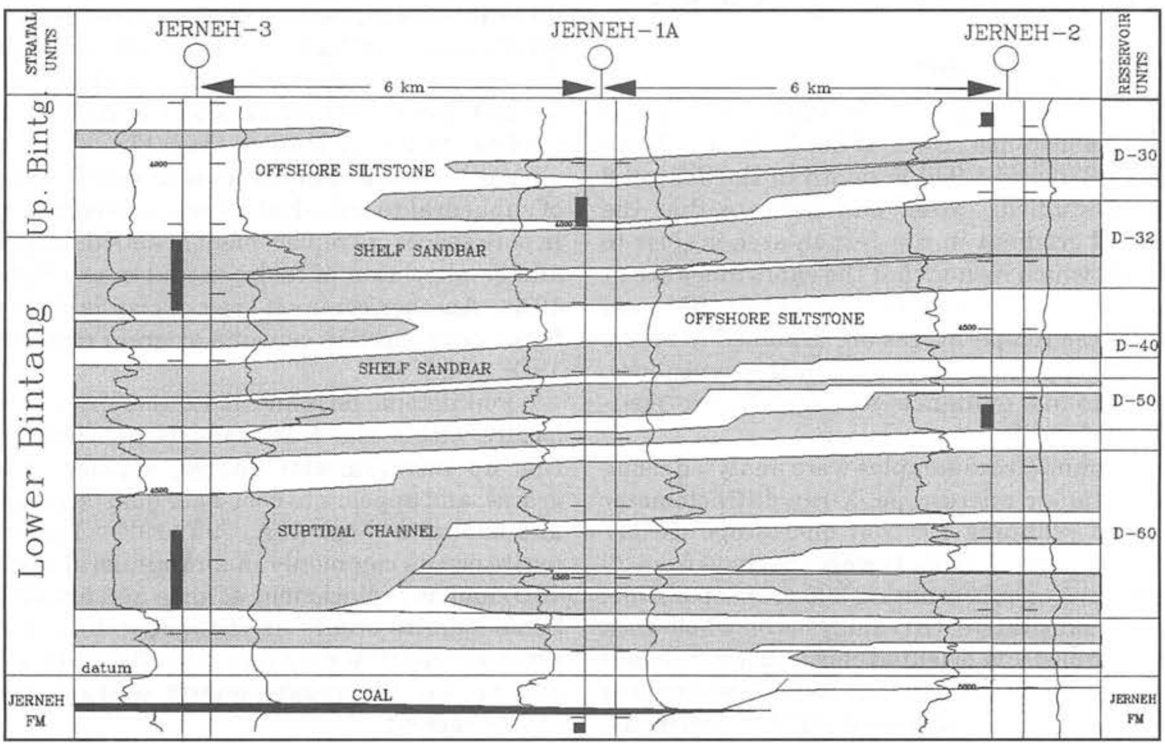

Figure 11. Correlation of shallow marine sandbodies in the lower Bintang. Note the sheet-like geometry of most sandstones, and the similarly extensive shale beds. Core intervals are shown by the black bars.

I. Progradational phase

This phase resulted in the deposition of upward-coarsening delta front facies associations in the lower Jerneh formation. "Cyclic" repetition of the upward-coarsening sequences (15–20 m thick) was probably produced by switching of delta-lobes rather than relative sea-level changes. Each upward-coarsening cycle represents progradation of a delta lobe, and is overlain by the next progradational cycle as the lobe was abandoned and inundated by the sea. The sharp tops of coarsening-upward cycles are "marine flooding surfaces" which can be correlated across the entire field.

II. Aggradational phase

This depositional phase is represented by the upper Jerneh, which consists of coarsening- and fining-upward units of the delta plain facies association. During this phase, the rate of subsidence kept pace with the rate sedimentation, so that sea level was relatively stable. Sediment accumulation was primarily by vertical aggradation.

III. Transgressive phase

This phase is represented by the shallow marine facies association of the Bintang formation. It is interpreted to have occurred during a relative rise in sea level and transgression over the delta. The change from a sand-dominated to a mud-dominated sequence reflects the transgressive nature of this phase.

PETROGRAPHY AND DIAGENESIS

Materials and methods

For diagenetic studies, core samples from four reservoir sandstones (D-32, D-60, E-50, and E-90) between 1,270 and 1,940 m depth in the Jerneh-3 well were studied. Well data indicate that the geothermal gradient in the Jerneh area is close to 6°C/100 m, which means that the sandstones are at temperatures between approximately 95° and 135°C. These temperatures are assumed to be the maximum temperatures attained by the sandstones, as there is no evidence for significant post-depositional uplift.

More than 50 core samples were analysed using the petrographic microscope, X-ray diffractometer (XRD), and scanning electron microscope (SEM). Mineralogical data (Table 1) were obtained from 29 thin sections by point-counting 300 grains per slide.

Semi-quantitative XRD analyses on whole-rock powder samples and oriented clay (< 2 μm fraction) samples were done following the procedures adapted from Wilson (1987) and Griffin (1971). Generally, there is a good agreement between the results of XRD analysis (Table 2) and the results of thin section analysis, as shown graphically in Figure 13.

Detrital mineralogy

The sandstones are well to moderately well sorted and silty to very fine-grained (mean grain size: 60–100 μm). The detrital quartz grains are mostly subangular to angular. In terms of framework mineralogy, the sandstones are classified as subfeldspathic arenites or sublitharenites (Fig. 14), their framework composition being: quartz (71–84%), feldspars (6–19%), and rock fragments (4–18%). Some feldspar grains are partially dissolved (Figs. 15B, 15C) or are altered to secondary clay minerals. The amount of K-feldspar appears to decrease steadily with increasing depth (Fig. 16).

Clay generally constitute 2–11% of total rock, although some bioturbated sandstones in the D-32 have up to 25% clay matrix. XRD analyses indicate that the clays are mainly kaolinite and illite. Chlorite and expandable clays are more common in the D-32 sandstones (shallow marine), while kaolinite is more abundant in the E-50 and E-90 (nonmarine).

Authigenic cements and clay minerals

Quartz overgrowths increase with increasing depth, ranging from 1 to 11% of total rock (Fig. 16). The D-32 sandstones contain < 2% overgrowths whereas the deeper E-50 and E-90 sandstones have up to 10% overgrowths. SEM studies indicate that quartz overgrowths in the D-32 sandstones are in the early stages of growth, whereas those in the E-50 and E-90 sandstones are well-developed and tend to block pore throats (Fig. 17).

Authigenic kaolinite occurs as vermiform stacks of subhedral to euhedral pseudohexagonal crystals in pore spaces, as replacement of detrital clay clasts, and as alteration of feldspar and mica (Figs. 18B, 19A). Another common type of clay is illite which forms meniscus-like cements at grain contacts (Fig. 19D).

Poikilotopic ferroan calcite cement occurs only locally within the E-90 sandstone. This cement fills up intragranular spaces, replaces feldspar grains, and appears to post-date quartz overgrowth and kaolinite (Figs. 18A, 19E, 19F). Framboydal pyrite occurs commonly in foraminiferal tests (Fig. 18D) and as replacement of mica and matrix clays. Some siderite occurs as rhombs, < 10 μm across, replacing detrital clay and mica flakes (Fig. 18C), and appear to predate quartz overgrowths and calcite cement.

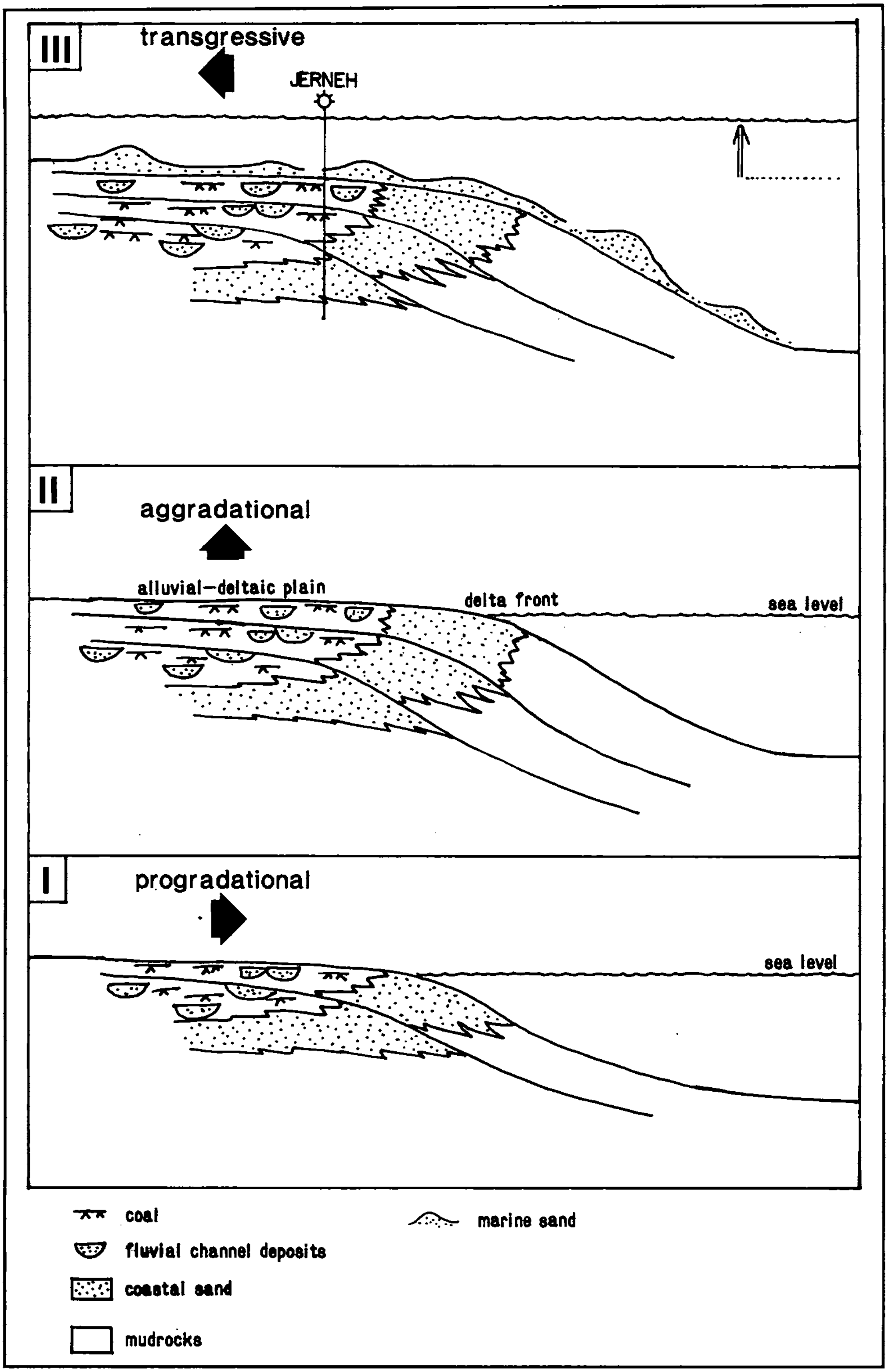

Figure 12. Summary of the depositional history of the Jerneh field reservoir interval. I. Progradation produces the coarsening-upward sequences in lower Jerneh. II. Aggradation of the delta plain as the rate of subsidence and rate of sedimentation is balanced. III. Transgressive sedimentation over the delta due to rise in relative sea level, resulting in shallow marine sandbodies.

Table 1. Mineralogical composition of sandstones in the Jerneh-3 well, determined by point-counting 300 grains per sample. Figures are in % of total rock (minus pore space).

FORMATION	BINTANG							BINTANG				
RESERVOIR UNIT	D-32							D-60				
SAMPLE NO.	1	2	3	4	5	6	7	8	9	10	11	12
Quartz	56	51	51	50	50	41	55	58	48	51	51	42
Polyquartz	3	9	10	15	10	8	10	11	12	9	8	7
Chert	4	5	5	4	4	1	3	3	4	1	2	5
Feldspar	9	7	11	8	8	7	8	5	14	14	10	12
Rock fragments												
• Sedimentary	7	5	4	9	8	1	5	6	5	4	6	3
• Metamorphic	3	2	4	3	1	1	2	1	1	4	2	1
• Igneous	–	–	–	–	–	–	–	–	–	–	–	–
Mica	5	5	3	2	2	3	5	3	5	3	2	5
Matrix	7	8	6	4	12	32	6	8	8	9	10	12
Heavy Minerals	1	1	1	1	–	1	1	2	–	1	1	1
Glauconite	–	1	2	2	4	2	2	–	–	–	–	–
Detrital Carbonate	–	2	1	–	1	–	–	–	–	–	–	–
Carbonaceous material	–	2	–	–	–	2	–	–	–	–	2	2
Quartz Overgrowth	1	2	2	1	1	1	2	3	3	3	5	4
Kaolinite	–	1	–	–	–	–	–	–	–	1	–	–
Illite	–	–	–	–	–	–	–	–	–	–	–	–
Chlorite	1	–	–	1	–	–	–	–	–	–	–	–
Calcite	–	–	–	–	–	–	–	–	–	–	–	–
Dolomite	–	–	–	–	–	1	2	–	–	–	–	–
Siderite	–	–	–	–	–	1	–	–	–	–	2	5
Pyrite	2	–	–	–	–	1	–	–	–	–	–	–
Porosity (% Bulk vol.)	35	34	31	31	28	20	39	34	28	22	30	21

FORMATION	JERNEH							JERNEH									
RESERVOIR UNIT	E-50							E-90									
SAMPLE NO.	13	14	15	16	17	18	19	20	21	22	23	24	25	26	27	28	29
Quartz	61	64	61	46	61	52	51	53	52	65	57	56	50	50	39	55	53
Polyquartz	1	5	6	6	6	12	8	5	8	5	6	3	7	1	5	6	8
Chert	–	3	1	–	2	2	–	–	1	3	2	2	1	1	3	3	1
Feldspar	13	8	8	9	6	8	14	16	14	6	7	6	6	10	3	5	8
Rock fragments																	
• Sedimentary	3	3	4	6	7	6	4	6	5	5	3	6	9	3	6	6	8
• Metamorphic	–	1	1	1	1	1	–	–	1	–	1	–	–	–	–	–	1
• Igneous	–	–	–	–	–	–	–	–	–	–	–	–	–	–	–	–	–
Mica	4	2	2	5	2	3	3	2	2	1	3	4	1	5	–	–	1
Matrix	7	6	4	15	6	6	10	7	6	6	10	8	12	14	2	8	4
Heavy Minerals	–	–	1	2	2	1	1	1	1	2	1	1	1	1	–	1	1
Glauconite	–	–	–	–	–	–	–	–	–	–	–	–	–	–	–	–	–
Detrital Carbonate	–	–	–	–	–	–	–	–	–	–	–	–	1	1	–	–	–
Carbonaceous material	5	–	–	–	–	–	–	–	–	–	–	–	–	3	–	–	1
Quartz Overgrowth	1	7	10	8	6	8	9	9	6	6	7	10	5	6	–	4	6
Kaolinite	1	1	1	–	1	1	–	1	2	–	1	1	2	3	–	2	–
Illite	–	–	1	–	–	–	–	–	–	–	–	–	1	–	–	–	–
Chlorite	–	–	–	–	–	–	–	–	–	–	1	–	–	–	–	–	–
Calcite	–	–	–	–	–	–	–	–	–	–	–	–	–	–	33	–	–
Dolomite	–	–	–	–	–	–	–	–	–	–	–	–	–	–	–	–	–
Siderite	3	–	–	1	–	–	–	1	2	1	1	4	4	2	8	8	9
Pyrite	–	–	–	–	–	–	–	–	–	–	–	–	–	–	–	–	–
Porosity (% Bulk vol.)	35	30	25	29	28	29	31	25	27	25	20	22	22	20	0	24	26

Sample No.	Depth/m RKB	Sample No.	Depth/m RKB	Sample No.	Depth/m RKB
1.	1256.6	11.	1412.8	21.	1935.8
2.	1260.3	12.	1414.6	22.	1936.8
3.	1263.0	13.	1717.8	23.	1937.7
4.	1264.8	14.	1736.4	24.	1938.6
5.	1266.7	15.	1738.2	25.	1938.7
6.	1268.5	16.	1740.9	26.	1941.3
7.	1284.1	17.	1741.8	27.	1941.9
8.	1387.8	18.	1741.9	28.	1943.2
9.	1408.8	19.	1745.5	29.	1944.1
10.	1409.1	20.	1935.2		

Diagenetic history

The diagenetic sequence in the sandstones was interpreted from the textural relationships between authigenic minerals (Fig. 20). The sequence consists of two stages — shallow (0–1,200 m of burial) and intermediate (1,200–2,000 m).

0–1,200 m

This shallow burial stage is dominated by microbial diagenetic processes (e.g. Curtis, 1978) which resulted in the formation of pyrite, siderite, and calcite. The volume of these early cements is < 4%, which suggests that porosity reduction during shallow burial was mainly caused by mechanical compaction. Assuming that the initial porosity of the sandstones was 40% (cf. Houseknecht, 1987), it is estimated that about 15–50% of that porosity was lost during compaction by the reduction of primary intergranular porosity.

1,200–2,000 m

Further reduction of porosity occurred at depths greater than 1,200 m (Fig. 20). Quartz overgrowth probably started to form at about 1,200 m depth (approximately 90°C), and increases steadily from an average of 1% at 1,270 m to 7% at 1,940 m (Fig. 16). Dissolution of K-feldspar within the sandstones may have provided part of the silica for the overgrowths. XRD data (Table 2) indicate that an average of 6 vol. % K-feldspar had been dissolved. This would have formed only 2 vol. % authigenic quartz in the sandstones (Bjorlykke, 1984). The remaining 4 vol. % quartz overgrowth must have been derived from other sources, notably from clay

Table 2. Mineralogy from semi-quantitative whole-rock XRD analysis, Jerneh-3 cores (62 samples). All samples are sandstones except those labelled 'sh', which refers to mudstone/siltstone samples.

DEPTH/m	QUARTZ	ORTHO	PLAGIO	CALCITE	DOLOM	SIDERIT	PYRITE	MICA	KAOLIN
1256.60	67	10	5	-	-	-	-	13	5
1260.26	69	6	6	-	1	-	-	12	6
1263.00	70	7	5	-	-	-	-	11	6
1264.84	63	11	5	-	1	-	-	15	6
1266.66	65	8	6	-	1	1	-	13	6
1268.50	59	12	5	-	1	-	1	14	7
1270.32	57	7	6	1	1	-	-	19	8
1272.16	48	10	7	-	2	1	-	22	10
1273.98sh	29	6	7	-	1	1	-	41	16
1274.90sh	28	6	5	-	1	1	-	42	16
1276.42	51	6	7	-	1	1	-	25	10
1281.00	56	6	9	-	1	-	-	18	9
1284.05	69	8	8	-	1	-	-	10	5
1286.80	39	6	5	-	1	1	-	36	12
1387.75	74	6	7	-	-	1	-	8	4
1390.19	65	6	5	-	-	-	-	16	8
1390.80	56	6	5	-	1	1	-	23	8
1390.54	64	7	8	-	-	-	-	14	6
1397.51	76	6	5	-	-	-	-	9	3
1400.26	73	5	6	-	-	3	-	9	5
1403.92	76	6	5	-	-	-	-	7	5
1408.80	70	11	6	-	-	-	-	9	4
1412.76	68	7	8	-	1	-	-	11	5
1414.59	70	5	7	-	1	-	-	12	5
1416.42	64	7	6	-	-	1	-	17	6
1418.25sh	58	5	6	-	-	2	-	19	10
1717.76sh	49	-	4	-	-	5	-	31	11
1717.76	65	4	8	-	-	1	-	13	10
1722.64sh	34	6	-	-	1	-	-	36	23
1725.38sh	41	4	2	-	-	1	-	31	21
1726.61sh	31	4	2	-	-	1	-	40	22
1728.44sh	49	4	4	-	-	4	-	22	17
1729.04sh	40	5	4	-	-	1	-	31	19
1736.36	76	5	3	-	-	-	-	9	7
1738.20	82	4	5	-	-	1	-	5	3
1740.02	64	8	6	-	-	1	-	14	7
1740.94	65	7	6	-	-	-	-	15	7
1741.86	74	5	5	-	-	4	-	8	4
1743.68	61	5	15	-	-	1	-	13	5
1745.52	72	6	6	-	-	-	-	10	5
1747.34	65	6	6	-	-	3	-	12	7
1748.56	70	5	6	-	-	-	-	11	7
1749.18	60	3	8	-	-	2	-	19	8
1751.00sh	40	4	4	-	-	1	-	39	12
1930.34sh	42	5	6	-	-	1	-	31	15
1932.18sh	51	3	4	-	-	1	-	24	17
1933.40sh	42	4	4	-	-	1	-	33	15
1934.00sh	59	4	4	-	-	1	-	16	16
1935.22	79	3	6	-	-	-	-	6	6
1935.84	67	4	5	-	-	2	-	12	10
1936.75	72	3	7	-	-	1	-	13	4
1937.66	66	4	6	-	2	1	-	13	9
1938.58	79	-	5	-	-	1	-	10	6
1939.50	84	-	4	-	-	-	-	5	6
1941.32	74	3	6	-	-	1	-	10	6
1941.94	64	2	4	21	-	-	-	5	3
1942.24	64	-	4	22	-	1	-	6	3
1943.16	78	3	5	-	-	1	-	7	7
1944.07	82	2	5	-	-	-	-	6	5
1945.90sh	53	-	8	-	-	1	-	28	10
1946.82sh	48	-	7	-	-	1	-	31	13
1947.73	36	5	6	-	-	1	-	38	15

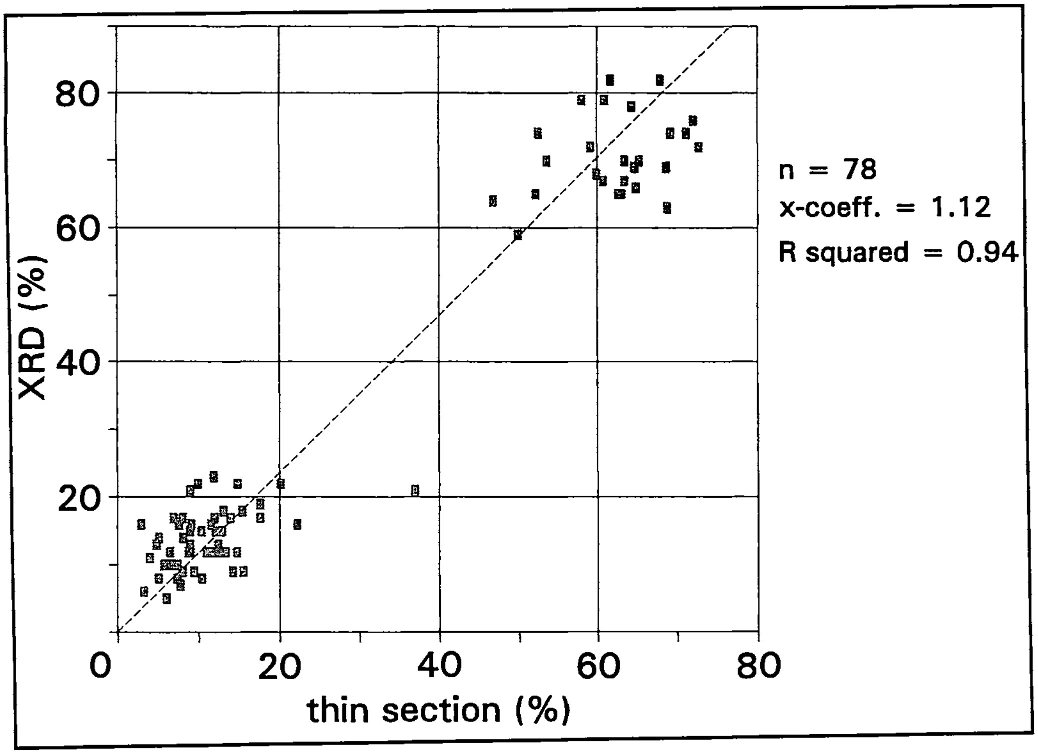

Figure 13. Graphical representation of comparison made between the mineralogical data from XRD and those obtained by thin section analyses.

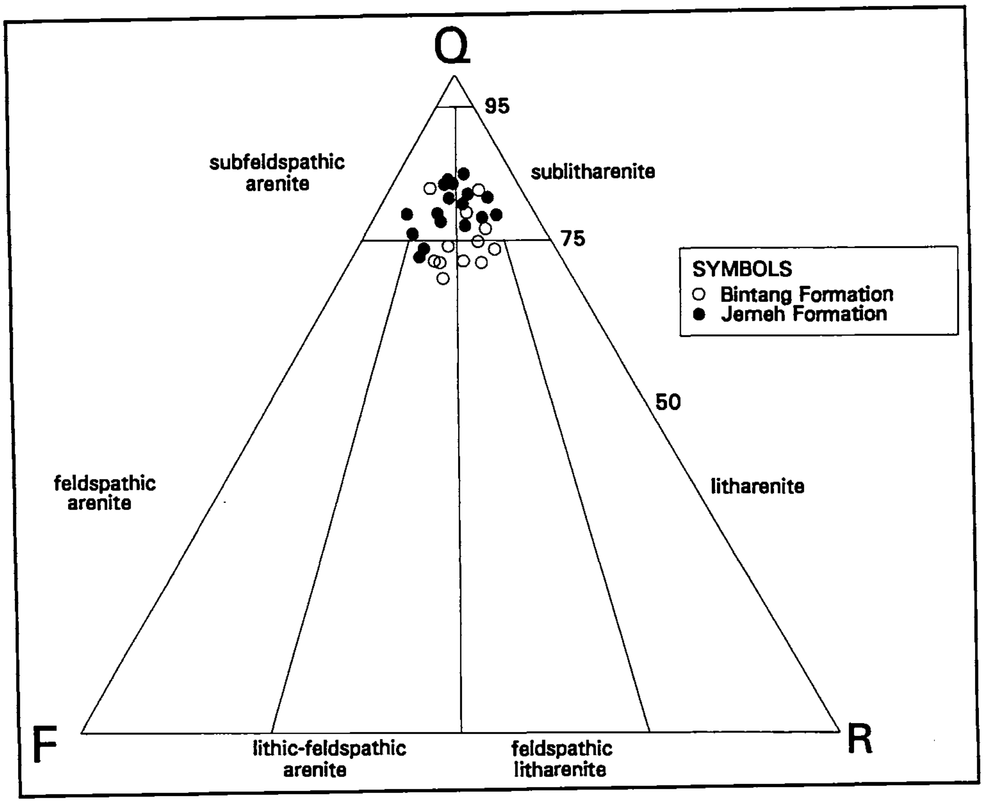

Figure 14. Triangular plot of framework composition of sandstones based on thin section data. Nomenclature of Folk (1980).

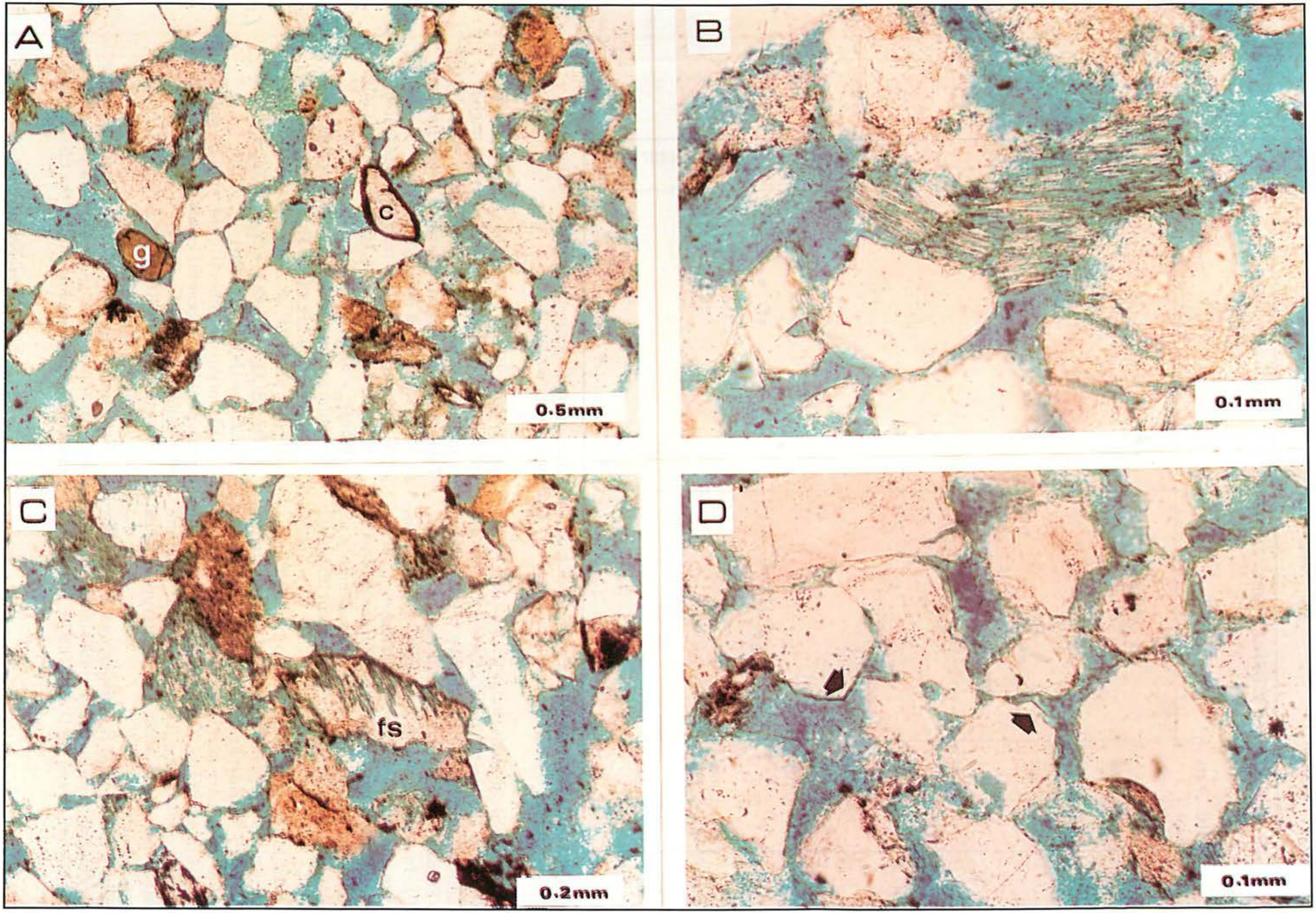

Figure 15. Thin section photomicrographs. A) Porous, very fine-grained, well-sorted sandstone, containing glauconitic grain (g), limestone clast (c), and pore-lining clays (upper right corner). D-32 sandstone, 1,263 m. B) At centre of photo is a feldspar grain that has been dissolved and slightly deformed by compaction. D-60 sandstone, 1,408.8 m. C) Moderately sorted fine to very fine grained sandstone with partially dissolved feldspar grains (fs). D-60 sandstone, 1,408.8 m. D) Abundant quartz overgrowths with euhedral terminations (arrows). E-50 sandstone, 1,738.2 m.

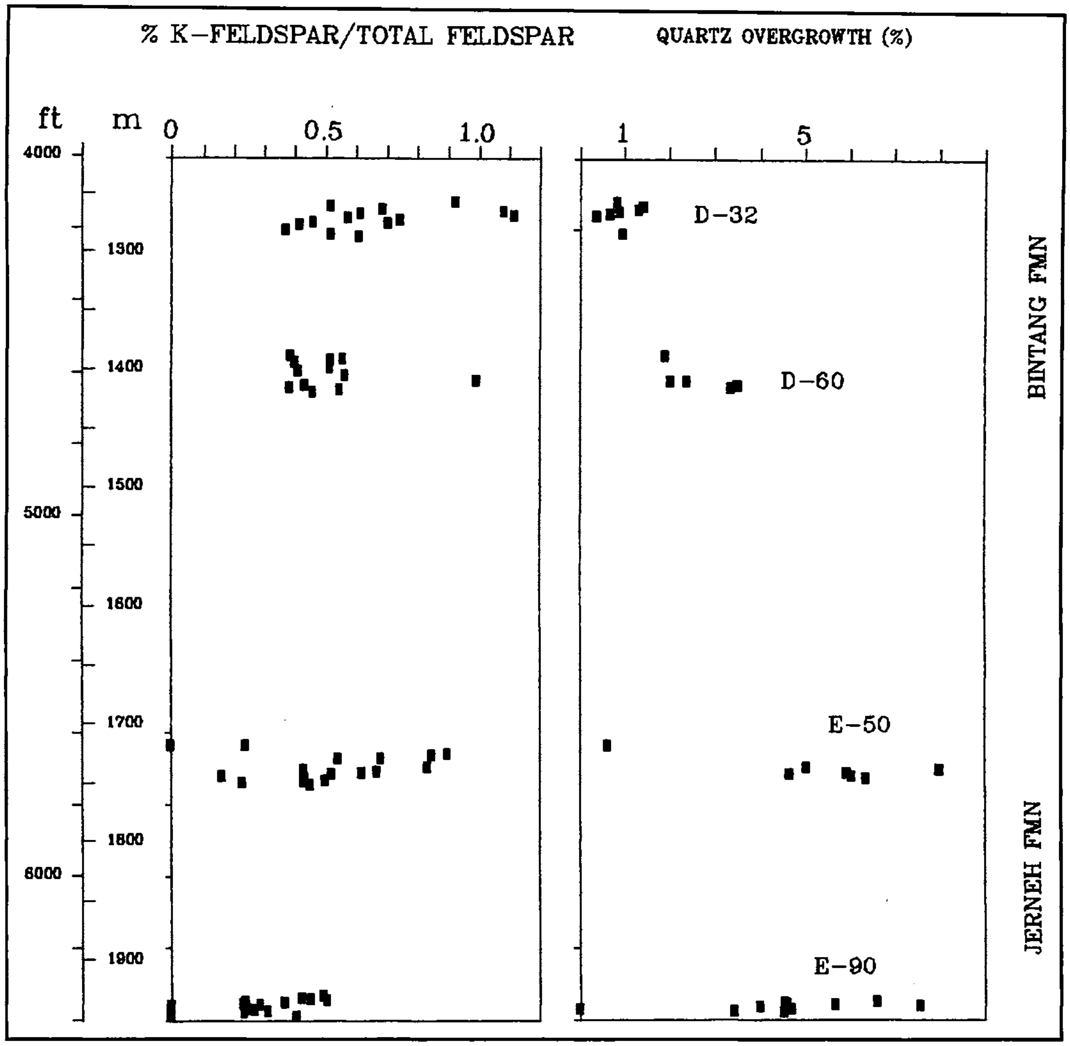

Figure 16. Depth plots showing the increase in quartz overgrowth (thin section data) concomitant with the loss of K-feldspar (from whole-rock XRD analyses) during burial.

reactions in the adjacent shales (Boles and Franks, 1979), since the interval of study now lies within the smectite-to-illite transformation window (Boles and Franks, 1979; Dypvik, 1983; Freed and Peacor, 1989). In a recent world-wide study of sandstones, Gluyas and Coleman (1992) have shown that the silica content of sandstones increases during diagenesis, suggesting that silica cements in sandstones are mainly derived from external sources.

Dissolution of K-feldspar also resulted in the formation of authigenic kaolinite in the sandstones. The 6 vol. % K-feldspar dissolved within the study interval could account for only 3 to 4 vol. % authigenic kaolinite (Bjorlykke, 1984). The remaining half of the 6–7 vol. % total kaolinite (Table 2) in the sandstones is thus interpreted to be of detrital origin.

The dissolution of K-feldspar was achieved by CO_2-rich acidic pore fluids generated in the adjacent shales (Schmidt and McDonald, 1979; Lundegard and Trevena, 1987). Plagioclase feldspar, however, was relatively stable, as indicated by the negligible change in the amount of plagioclase with depth (Table 2). This suggests that K-feldspar had been selectively dissolved during burial.

K-feldspar dissolution may be represented as:

$2KAlSi_3O_8 + 2H_2CO_3 + H_2O = Al_2Si_2O_5(OH)_4 + 4H_4SiO_4 + 2HCO^{3-} + 2K^+$ .... (i)

Similarly, plagioclase dissolves as follows:

$2NaAlSi_3O_8 + 2H_2CO_3 + H_2O = Al_2Si_2O_5(OH)_4 + 4H_4SiO_4 + 2HCO^{3-} + 2Na^+$ .... (ii)

$CaAl_2Si_2O_8 + 2H_2CO_3 + H_2O = Al_2Si_2O_5(OH)_4 + 2HCO^{3-} + Ca^{2+}$ .... (iii)

Illitization of smectite in shales may be represented by the general equation (Hower *et al.*, 1976; Boles and Franks, 1979):

Smectite $+ Al^{3+} + K^+ + H_2O =$ illite $+ Si^{4+} + Na^+ + Ca^{2+} + Fe^{2+} + Mg^{2+} + H_2O$ .... (iv)

Equation iv indicates that an increase in the concentration of Na^+ and Ca^{2+} cations due to smectite illitization would inhibit the dissolution of

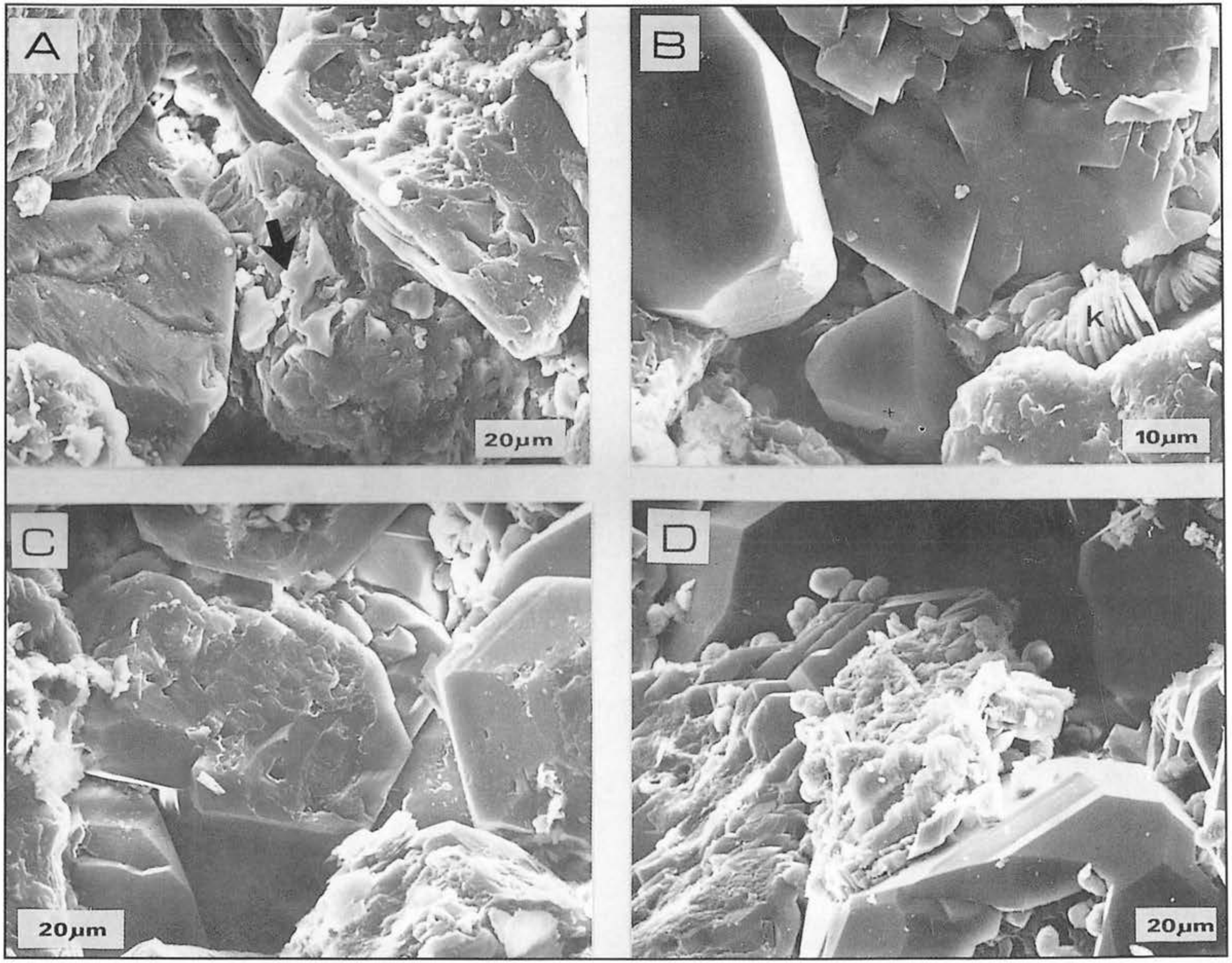

Figure 17. SEM photomicrographs showing quartz overgrowths in different reservoir sandstones. A) Incipient overgrowths (arrow), 1 vol. % overgrowths, D-32, 1,263 m. B) Well-developed overgrowths with euhedral terminations, 2 vol. % overgrowths, D-60, 1,408.8 m. C) Tight packing and restricted pore throats due to quartz overgrowths. 5 vol. % overgrowths, E-50, 1,741.9 m. D) Well developed overgrowths as in previous photograph. 5 vol. % overgrowths. E-90, 1,944.1 m.

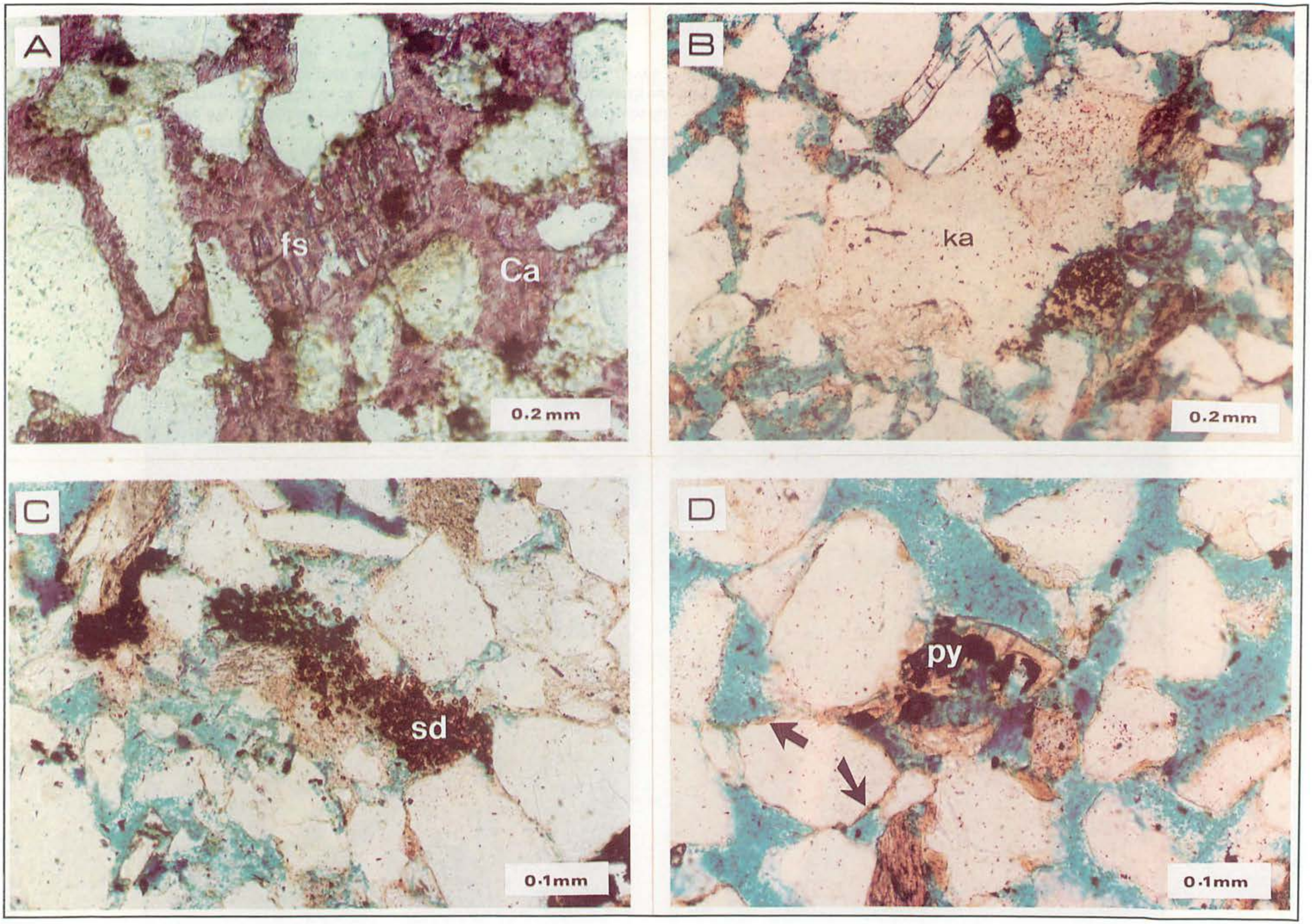

Figure 18. Photomicrographs. A) Ferroan calcite (Ca) cementing sand grains. Skeletal feldspar grain at centre (fs). 1,941.9 m. B) Large patch of detrital kaolinitic clast (ka) in D-60 sandstone. 1,409.1 m. C) Microcrystalline siderite (sd) replaces detrital clay matrix. 1,408.8 m. D) D-32 sandstone with foraminiferal test filled with framboydal pyrite (py). Arrows point to thin clay coatings on quartz grains, which give the rock a greenish colour. 1,268.5 m.

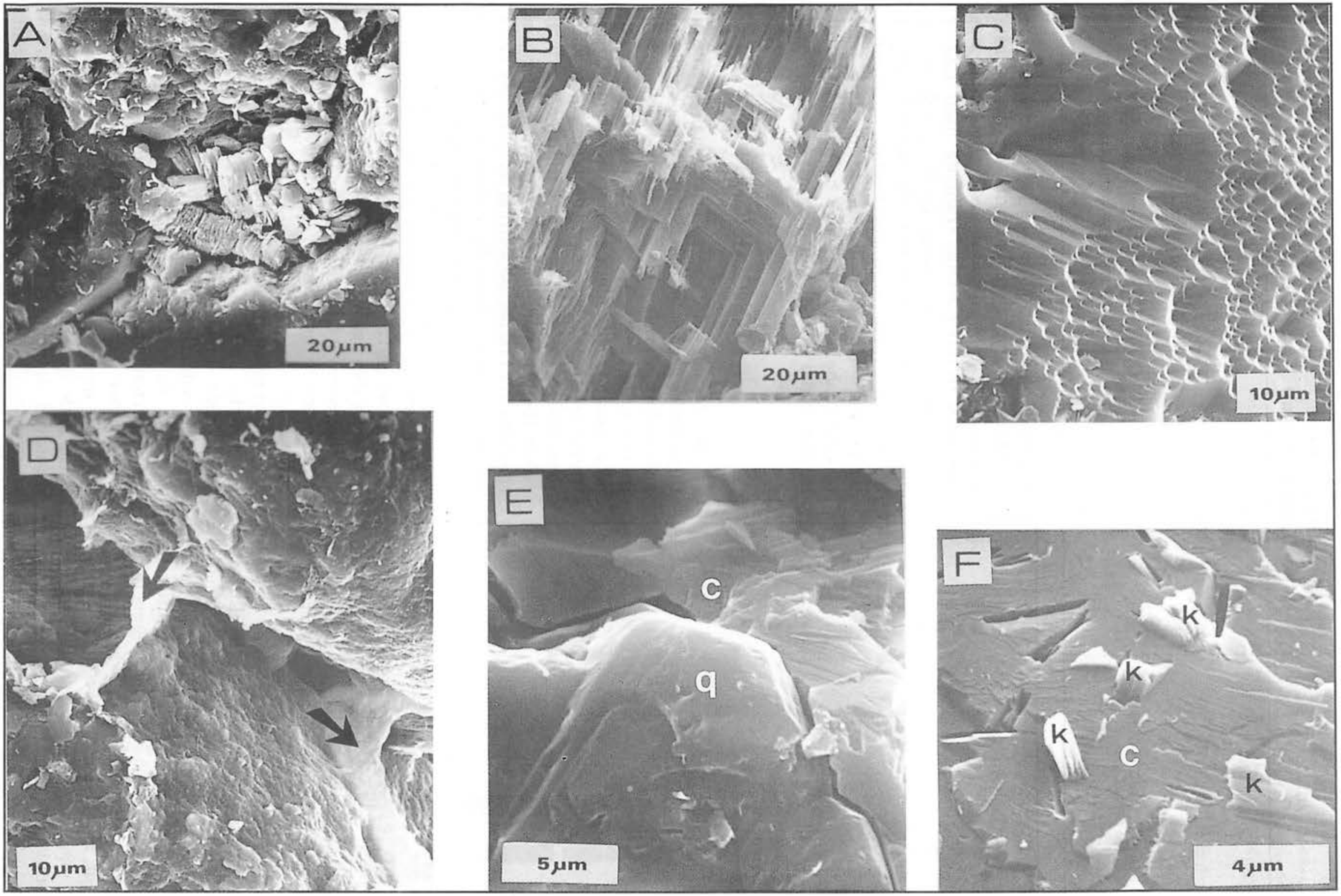

Figure 19. SEM photomicrographs showing some of the diagenetic features. A) Authigenic kaolinite in pore space. D-60 sandstone, 1,408.8 m. B) Skeletal K-feldspar grain produced by dissolution. D-60 sandstone, 1,408.8 m. C) Etch pits on surface of quartz grain, probably produced by aggressive pore fluids at depth. D-60 sandstone, 1,408.8 m. D) Pore-bridging meniscus illite (arrows). D-60 sandstone 1,263 m. E) Ferroan calcite (c) encloses quartz overgrowth (q). E-90 sandstone, 1,941.9 m. F) Ferroan calcite (c) encloses kaolinite (k). 1,941.9 m.

Table 3. Porosity gradients of selected basins compiled from the literature.

Basin (age)	Porosity gradient –% per 1,000 ft (300 m)	Reference
Texas Gulf Coast (Tertiary)	1.23	Loucks *et al.*, 1974
North Sea (Jurassic)	2.2-2.9	Selley, 1978; Bjorlykke *et al.*, 1986
East Texas (L. Cretaceous)	2.85	Dutton and Diggs, 1992
Pattani Basin (Tertiary)	3.5	Trevena and Clarke, 1986

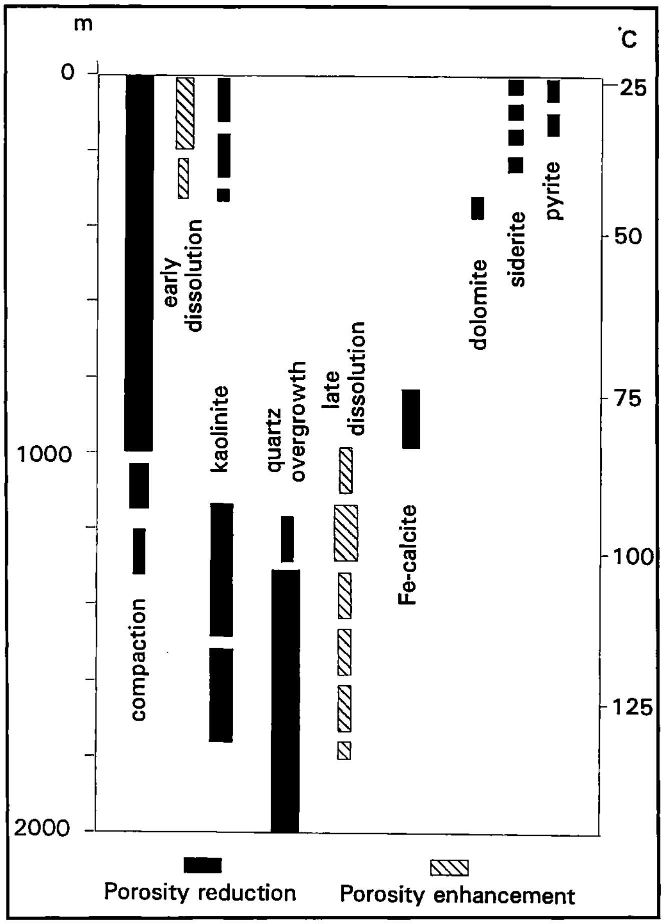

Figure 20. Sequence of diagenetic events and their relationships to porosity enhancement and reduction.

plagioclase (by driving equation ii and iii to the left). K^+ uptake by smectite during the illitization process (equation iv) would, however, increase the rate of K-feldspar dissolution. This explains why K-feldspar was more susceptible to dissolution than plagioclase. The same phenomenon seems to have occurred in the Pattani Basin where complete dissolution of K-feldspar occurred at shallower depths than plagioclase (Trevena and Clark, 1986; Lundegard and Trevena, 1990).

The dissolution of K-feldspar did not cause a significant increase in the porosity because of continued compaction as well as the precipitation of authigenic quartz and kaolinite. The higher rate of porosity loss with depth in the Jerneh sandstones compared to other basins (ranging from 1.23 to 3.8%/1,000 ft, Table 3) may be due partly to the higher geothermal gradient in the Malay Basin. In basins that have high geothermal gradients, temperature-dependent diagenetic reactions tend to occur at shallower burial depths, and may result in more rapid reduction in porosity.

CONCLUSIONS

The Jerneh field reservoir sandstones occur in three facies associations: delta front, delta plain, and shallow marine. These facies association are interpreted to represent periods of delta progradation, delta plain aggradation, and marine transgression, respectively. The major sandbodies show different degrees of lateral continuity, which reflect their depositional environments. Those in the delta front facies association have limited areal extent and thins laterally rather rapidly. The shallow marine sandbodies generally have sheet-like geometry, and are therefore of greater lateral extent. Channel sandbodies are, by nature, long and narrow, and thus will require detailed analysis to predict their geometries.

Diagenesis of the Jerneh field sandstones is interpreted to have involved mainly mechanical compaction during the first 1,200 m of burial, followed by relatively small amounts of cementation by quartz and kaolinite at deeper burial. Compaction during shallow diagenesis caused a 15–50% reduction of the original depositional porosity. At depths greater than 1,200 m, where formation temperatures exceeded 90°C, the porosity was further reduced to its present values of 10–25% by quartz and kaolinite cementation. Authigenic quartz derived its silica partly from dissolved detrital K-feldspar and partly from smectite-to-illite transformation in the adjacent shales. Dissolution of detrital K-feldspar also resulted in the precipitation of authigenic kaolinite.

ACKNOWLEDGEMENTS

This paper is based on a M.Sc. thesis submitted at the University of Malaya and supervised by Dr. Azhar Hj. Hussin and Prof. C.S. Hutchison of the Department of Geology. I would like to thank PETRONAS for granting permission to use the data, samples, and laboratory facilities for the study. I am especially grateful to Dr. Khalid Ngah and Dr. Ibrahim Komoo for their managerial support towards the completion of this work.

REFERENCES

ARMITAGE, J.H. AND VIOTTI, C., 1977. Stratigraphic nomenclature — southern end Malay Basin. *Proc. Indonesian Petrol. Assoc. 6th Ann. Conv.*, 69–94.

BJORLYKKE, K., 1984. Formation of secondary porosity: how important is it? *In:* McDonald, D.A. and Surdam, R.C. (Eds.), *Clastic Diagenesis*. Am. Assoc. Petrol. Geol. Mem. 37, 277–286.

BJORLYKKE, K., AAGARD, P., DYPVIK, H., HASTINGS, D.S. AND HARPER, A.S., 1986. Diagenesis and reservoir properties of Jurassic sandstones from the Haltenbanken area, offshore mid-Norway. *In: Habitat of Hydrocarbons in the Norwegian Continental Shelf*. Norwegian Petroleum Soc., Graham and Trotman, 275–286.

BOLES, J.R. AND FRANKS, S.G., 1979. Clay diagenesis in Wilcox

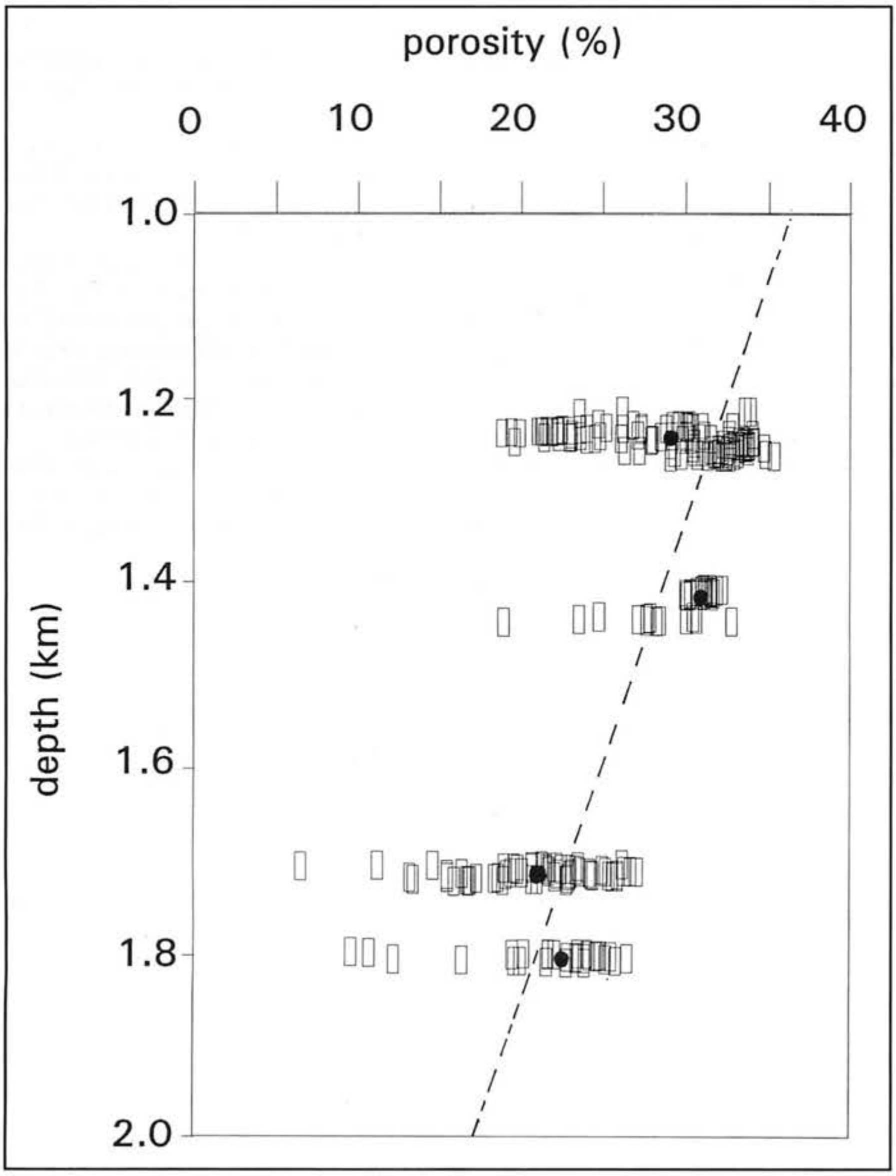

Figure 21. Plot of porosity vs depth for the reservoir sandstones in the Jerneh field, based on core analysis data.

sandstones of southwest Texas: implications of smectite diagenesis on sandstone cementation. *Jour. Sed. Petrology*, 49, 55–70.

BOYLES, J.M. AND SCOTT, A.J., 1982. A model for migrating shelf bar sandstones in Upper Mancos Shale (Campanian), Northwestern Colorado. *Am. Assoc. Petrol. Geol. Bull.*, 66, 491–508.

CURTIS, D.M., 1970. Miocene deltaic sedimentation, Louisiana Gulf Coast. *In:* Morgan, J.P. (Ed.), *Deltaic Sedimentation Modern and Ancient*. Spec. Publ. Soc. Econ. Paleont. Miner., 15, 293–308.

CURTIS, C.D., 1978. Possible links between sandstone diagenesis and depth-related geochemical reactions in enclosing mudstones. *Jour. Geol. Soc. London*, 135, 107–118.

DUTTON, S.P. AND DIGGS, T.N., 1992. Evolution of porosity and permeability in the Lower Cretaceous Travis Peak Formation, East Texas. *Am. Assoc. Petrol. Geol. Bull.*, 76, 252–269.

DYPVIK, H., 1983. Clay mineral transformations in Tertiary and Mesozoic sediments from the North Sea. *Am. Assoc. Petrol. Geol. Bull.*, 67, 160–165.

ELLIOTT, T., 1986. Deltas. *In:* Reading, H.G. (Ed.), *Sedimentary Environments and Facies*. 2nd Ed., Elsevier, New York, 97–142.

FOLK, R.L., 1980. *Petrology of Sedimentary Rocks*. Hemphill, Austin Texas, 123–127.

FREED, R.L. AND PEACOR, D.R., 1989. Variability in temperature of the smectite/illite reactions in Gulf Coast sediments. *Clay Miner.*, 24, 171–180.

GLUYAS, J. AND COLEMAN, M., 1992. Material flux and porosity changes during sediment diagenesis. *Nature*, 356, 52–54.

GRIFFIN, G.M., 1971. Interpretation of X-ray diffraction data. *In:* Carver, R.E. (Ed.), *Procedures in Sedimentary Petrology*. Wiley Interscience, Toronto, 541–569.

HOUSEKNECHT, D.W., 1987. Assessing the relative importance of compaction processes and cementation to reduction of porosity. *Am. Assoc. Petrol. Geol. Bull.*, 71, 633–642.

LOUCKS, R.G., DODGE, D.M. AND GALLOWAY, W.E., 1984. Regional controls on diagenesis and reservoir quality in lower Tertiary sandstones along the Texas Gulf Coast. *In:* McDonald, D.A. and Surdam, R.C. (Eds.), *Clastic Diagenesis*. Am. Assoc. Petrol. Geol. Mem. 37, p. 15–45.

LUNDEGARD, P.D. AND TREVENA, A.S., 1987. Influence of fluid chemistry and high geothermal gradient on sandstone diagenesis: Pattani Basin, Gulf of Thailand. *Am. Assoc. Petrol. Geol. Bull.*, 71, 586 (abstract).

LUNDEGARD, P.D. AND TREVENA, A.S., 1990. Sandstone diagenesis in the Pattani Basin (Gulf of Thailand): history of water-rock interaction and comparison with the Gulf of Mexico. *Applied Geochem.* 5, 669–685.

NIK RAMLI, 1988. Development of a humid tropical fan-delta system: the middle Tertiary 'K' sandstone in the southeastern Malay Basin, offshore West Malaysia. *In:* Nemec, W. and Steel, R.J. (Eds.), *Fan Deltas: Sedimentology and Tectonic Settings*, Blackie, Glasgow, 341–353.

SCHMIDT, V. AND MCDONALD, D.A., 1979. The role of secondary porosity in the course of sandstone diagenesis. *In:* Scholle, P.A. and Schluger, P.R. (Eds.), *Aspects of Diagenesis*. Soc. Econ. Paleont. Miner. Sp. Publ. 26, 175–207.

SELLEY, R.C., 1978. Porosity gradients in North Sea oil-bearing sandstones. *Jour. Geol. Soc. London*, 135, 119–132.

THAMBYDURAI, R., MUSTAFFA, A.F., MUELLER, K.H. AND DIXON, M.R., 1988. Jerneh Gas Field development planning. *7th offshore South East Asia Conf.*, Singapore, 2–5 February 1988, 859–870.

THIRAMONGKOL, N., 1983. Geomorphology of the Lower Central Plains, Thailand. *Proc. 3rd Meeting Working Gp. on Geomorphology of Rivers and Coastal Plains*. Bangkok, Thailand, 11–17 December 1983, 13–25.

TREVENA, A.S. AND CLARK, R.A., 1986. Diagenesis of sandstone reservoirs of Pattani Basin, Gulf of Thailand. *Am. Assoc. Petrol. Geol. Bull.*, 70, 299–308.

WILSON, M.J., 1987. X-ray powder diffraction methods. *In:* Wilson, M.J. (Ed.), *A Handbook of Determinative Clay Mineralogy*. Blackie, Glasgow, 89–98.

Manuscript received 4 March 1993

APPENDIX — Symbols

LITHOLOGY

- sandstone
- interbedded sandstone-mudstone
- mudstone
- coal
- pebbles

GRAIN SIZE

c	clay
s	silt
vf	very fine sand
f, fs	fine sand
m	medium sand
cs	coarse sand

SEDIMENTARY STRUCTURES

- parallel lamination
- cross lamination
- wavy bedding
- convolute bedding
- flaser bedding
- herring-bone cross lamination
- burrows
- bioturbation
- load cast
- plant fragments
- root casts
- foraminifer
- slumps